London (1979–1984) and the Fuel Cells Group, Materials Research Department, Risø National Laboratory, Denmark have indirectly contributed to this section.

This section was written by N. Bonanos, B. C. H. Steele, and E. P. Butler and revised by N. Bonanos. The revised section is dedicated to the memory of B. C. H. Steele.

4.2 CHARACTERIZATION OF THE ELECTRICAL RESPONSE OF HIGH RESISTIVITY IONIC AND DIELECTRIC SOLID MATERIALS BY IMMITTANCE SPECTROSCOPY

J. Ross Macdonald

4.2.1 Introduction

For at least several decades, the effects of charged-particle motion in doped semiconductors, amorphous materials, polycrystals, single crystals, inorganic glasses, and polymers have been of much interest to both experimentalists and theorists. In fact, J. C. Phillips [1994] has characterized the problem of relaxation in complex disordered systems as the most important unsolved problem in physics! For ionically conducting materials such as solid electrolytes, the dynamics of the mobile ions have usually been investigated by analyzing the frequency response of the material over a wide range of frequencies, sometimes as wide or wider than 10^{-5} Hz to 10^{12} Hz. Such investigations thus usually involve immittance spectroscopy measurements and techniques. In this section, the main emphasis is on ionic conductors because of their technological importance in such areas as batteries, fuel cells, electrochromic displays, energy storage in capacitors, sensors, and even bionics. Because the electrical response of ionic conductors is rarely of simple Debye-relaxation character except in limiting cases, one must be concerned with its generalization: dispersive response.

Conductive-system dispersive response may be associated with a distribution of relaxation times (DRT) at the complex resistivity level, as in the work of Moynihan, Boesch, and Laberge [1973] based on the assumption of stretched-exponential response in the time domain (Eq. (118), Section 2.1.2.7), work that led to the widely used original modulus formalism (OMF) for data fitting and analysis. In contrast, dielectric dispersive response may be characterized by a distribution of dielectric relaxation times defined at the complex dielectric constant or permittivity level (Macdonald [1995]). Its history, summarized in the monograph of Böttcher and Bordewijk [1978], began more than a hundred years ago. Until relatively recently, however, these two types of dispersive response were not usually distinguished, and conductive-system dispersive response was often analyzed as if it were of dielectric character, even when this was not the case. In this section, material parameters will be expressed in specific form appropriate to the level concerned.

Conductive-system dispersion (CSD) usually involves thermally activated conduction extending to zero frequency plus an always-present bulk dielectric constant, $\varepsilon_{D\infty}$, usually taken to be frequency-independent in the experimental range. Dielectric-system dispersion (DSD) often involves dielectric-level response with only weak temperature dependence, and it may or may not involve a non-negligible frequency-independent leakage resistivity, $\rho_{C\infty} = \rho_{dc} \equiv \rho_0 \equiv 1/\sigma_0$. There may be cases where separate processes lead to the simultaneous presence within an experimental frequency range of both types of dispersion, but this is rare for most solid electrolytes. Further complications are present when conduction involves both mobile ionic and electronic charges, neither of whose effects are negligible (Jamnik [2003]). Here only ionic, dipolar, and vibronic effects will be further considered, with the main emphasis on conductive rather than on dielectric dispersion.

Since conductive-system dispersive response may be transformed and shown graphically at the complex dielectric level, and dielectric dispersion may be presented at the complex resistivity level, frequency-response data alone may be insufficient to allow positive identification of which type of process is present, since there may be great similarity between the peaked dispersion curves that appear in plots of $\rho''(\omega)$ and of $\varepsilon''(\omega)$ or of $\varepsilon_s''(\omega) \equiv \varepsilon''(\omega) - (\sigma_0/\omega\varepsilon_V)$. Here, ε_V is the permittivity of vacuum. This quantity has usually been designated as ε_0, as in other parts of this book. Its designation here as ε_V avoids ambiguity and allows clear distinction between it and $\varepsilon(0) = \varepsilon'(0) \equiv \varepsilon_0$, the usage in the present section.

Even CNLS data fitting at a specific temperature may not always allow unambiguous discrimination between CSD and DSD responses. But if data are available over a range of temperatures, discrimination is straightforward. Then, one generally finds that ρ_0/T (or ρ_0) and τ_σ, the characteristic relaxation time of a model exhibiting thermally activated CSD, involve the same activation enthalpy (usually termed the activation energy) (e.g. Macdonald [2002a]). This is an effective quantity when the process considered involves a distribution of activation energies. Dielectric dispersion response may not be thermally activated but when it is, τ_σ certainly does not have the same activation energy as that of an independent leakage resistivity ρ_0. A detailed study of discrimination between the two types of dispersion appears in Macdonald [1999a].

4.2.2 Types of Dispersive Response Models: Strengths and Weaknesses

4.2.2.1 Overview

Conductive-system dispersive response involving mobile charge may be conceptually associated with the effects of three processes:

1. electrode effects, which are particularly important at low frequencies (see Section 2.2.3.1) but may not be negligible at very high ones (Macdonald [2002a,b]);

2. ionic hopping effects, usually significant at mid-range frequencies (Macdonald [2002a,b]);
3. nearly constant loss effects primarily evident at sufficiently low temperatures over the usual frequency range or at high frequencies for higher temperatures (Ngai [1999], Ngai and León [2002], Macdonald [2002c, 2003b]).

Three different kinds of models have been proposed for describing these responses. A summary of some of the pertinent history of attempts to characterize the situation appears in Roling *et al.* [2001]. We shall consider here only models for the above behaviors that may be associated with mobile charge effects. The first and most desirable would be a fully microscopic model that accounted for all the above processes, since they are all directly or indirectly associated with mobile charge in conductive-system materials. Unfortunately, this many-body problem involving all interactions is currently insoluble.

A second approach involves approximate microscopic models whose log–log $\sigma'(\omega)$ slope continuously increases toward a value of unity until a high-frequency plateau is reached. No account of electrode effects is included in these approaches. In most other models, their high-frequency slope is related to a model parameter and quickly increases to a constant value less than unity as the frequency increases and before a final plateau begins to appear (Macdonald [1997b, 2002d]).

The third approach involves a composite model involving separate parts: one accounting for ionic hopping; a parallel contribution representing the effect of the endemic bulk dielectric constant, $\varepsilon_{D\infty}$; possibly a part describing nearly constant loss; and finally a series response model to account for electrode effects. For fitting most limited-range data, only two or three of these parts are usually required and excellent data fits are generally found using appropriate models. We shall therefore consider some composite models in detail.

It is noteworthy that most comparisons and fits of models to experimental data deal only with $\sigma'(\omega)$ response. An advantage of this procedure is that $\sigma'(\omega)$ and $\varepsilon''(\omega) \equiv \sigma'(\omega)/\omega\varepsilon_v$ are the only ones of the eight real and imaginary parts of the four immittance levels that are independent of the presence of $\varepsilon_{D\infty}$: $\sigma'(\omega)$ fitting is thus simpler than fitting with any of the four complex immittance-level responses or with the six other real and imaginary parts. Such an approach does not allow estimation of $\varepsilon_{D\infty}$, however, and it not only forfeits the error-averaging inherent in CNLS fitting but also the latter's test for the applicability of the Kronig–Kramers transformations.

The following discussion does not include consideration of all reasonable models that have been proposed and used for conductive-system fitting, but only some widely used ones and ones of particular theoretical importance.

4.2.2.2 *Variable-slope Models*

The Mismatch and Relaxation Model. Although some apparent theoretical defects inherent in the mismatch-and-relaxation model of Funke [1998], have been pointed out (Macdonald [1999b]), they have neither been explicitly recognized nor directly resolved. A recent empirical modification of this approach (Funke *et al.* [2002]) seems, however, to avoid some of the problems of the earlier work. Further,

new work of Funke and Banhatti [2004] corrects further weakness in the model, although it still contains some empirical elements and thus cannot be considered a full microscopic response model.

The Symmetric Hopping Model. This model (Dyre and Schrøder [2000]) ignores Coulomb interactions, claims to be of universal character in the extreme disorder limit, and yields response rather similar to that of the mismatch-and-relaxation model. Of the several approximate but specific microscopic hopping realizations of the microscopic model considered by Dyre and Schrøder, the diffusion-cluster-approximation one led to best results, although it involves low-frequency-limiting response in disagreement with the physically realistic dependencies of the real and imaginary parts of the ac conductivity on ω^2 and ω, respectively (Odagaki and Lax [1980], Macdonald [1996, 1997b, 2001a]. The mathematical complexities of both the mismatch-and-relaxation model and the diffusion-cluster-approximation one makes data fitting and the estimation of values of model parameters difficult, and thus no CNLS fitting of data to estimate such parameters seems to have been published so far.

Comparisons of the variable-slope models with real-part conductivity data have rarely involved responses with a variation of $\sigma'(\omega)/\sigma_0$ greater than three decades starting from a low-frequency experimental value of this ratio of nearly unity, and even for such a limited range they usually show increasing disagreement with experiment toward the high end of this ratio where the relative frequency is large. In contrast, the results of a PK1-model (defined in the next section) fit of accurate synthetic data calculated for the microscopic diffusion-cluster hopping model and involving a range of $\sigma'(\omega)/\sigma_0$ greater than seven decades yielded a value of S_F, the relative standard deviation of the fit, of less than 0.01 and showed no deviation between $\sigma'(\omega)/\sigma_0$ data and fit points on a log–log plot, as well as no apparent slope variation (Macdonald [2001b]).

It is therefore clear that since the variable-slope models have not been compared with data that would allow discrimination between their predictions and those of simpler composite models, the variable-slope approaches, while of theoretical interest, are currently less appropriate for data fitting and analysis than are simpler and well-fitting composite models.

4.2.2.3 Composite Models

The ZC Power-law Model. Although we discuss some single dispersive-response models here, in practice they must always take account of $\varepsilon_{D\infty}$ and of possibly some other effects as well and so the overall model is always composite. A frequently used fitting model is the ZARC one of Eq. (22), Section 2.2. It is now more often designated as the ZC and, when written at the complex conductivity level, it may be expressed as $\sigma(\omega) = \sigma_0[1 + (i\omega\tau^{ZC})\gamma_{ZC}]$, where $0 < \gamma_{ZC} \leq 1$. The exponent γ_{ZC} has often been written as n and is the high-frequency-limiting log–log slope of the model. It has usually been found to have a value in the range $0.6 \leq \gamma_{ZC} \leq 0.7$.

The real part of the ZC model has been termed Jonscher or universal dynamic response, but the word "universal" is inappropriate since CNLS fits with the ZC or

with its $\sigma'_{ZC}(\omega)$ part have been shown to be much poorer than those with other composite models (Macdonald [2000b, 2003a]). Finally, the identification of τ_{ZC}, or its real-part-fitting counterpart, as the inverse of the hopping radial frequency of the charge carriers has also been shown to be unsuitable (Macdonald [2003a]), and a more appropriate choice, the CK1 model, is discussed below.

OMF and CMF Kohlrausch Response Models. Consider now the general definition of the I_k normalized frequency response quantity of Eq. (3), Section 2.2, with $k = D$, 0, and 1. For $k = D$, U_k in that equation is the complex dielectric constant, $\varepsilon(\omega)$, and for the other two values, U_k is the complex resistivity, $\rho(\omega)$. Now I_k may be calculated from either a distribution of relaxations times or from a temporal correlation function: see Macdonald [1996, 2002d] and Section 2.1.2.3. Although the $\rho_{0\infty}$ and $\rho_{1\infty}$ quantities entering into the definition of U_0 and U_1 are usually either zero or negligibly small, they may be large enough to affect the frequency response of the model at very high frequencies (Macdonald [2002d]). They will be taken zero for most of the present work. Then it follows that we may write $\rho_0(\omega) = \rho_0 I_0(\omega)$ and $\rho_1(\omega) = \rho_0 I_1(\omega)$, where we ignore the distinction between ρ_{00} and ρ_{01}.

The stretched-exponential temporal response of Eq. (63), Section 2.1, a versatile and theoretically plausible correlation function, is one whose corresponding frequency behavior is now called Kohlrausch–Williams–Watts or just Kohlrausch [1854] model response, denoted here by Kk. It is also now customary to replace the α of the stretched-exponential equation by β or β_k, with $k = D$ or 0. The $k = D$ choice may be related to KD-model dispersive frequency response involving a distribution of dielectric relaxation (properly "retardation") times, and the $k = 0$ and 1 choices to two different distributions of resistivity relaxation times and thus to K0 and K1-model responses, respectively. Note that the β_1 parameter of the important K1 model is not directly related to stretched exponential temporal response, as are the other Kohlrausch models, but the DRTs of the K0 and K1 models are closely related (Macdonald [1997a]). Further, although the KD and K0 models are identical in form, they apply at different immittance levels and so represent distinct response behaviors.

No closed form expressions are available for the frequency responses of the Kk models for arbitrary β_k values but algorithms for calculating such responses and for fitting data with them are included in the free LEVM CNLS fitting program (Macdonald and Potter [1987], Macdonald [2000a]) and are very accurate for $0.3 \leq \beta_k \leq 0.7$ and somewhat less accurate outside this range. Further, LEVM also includes closed-form exact-response expressions for the choices $\beta_k = 1/3$ and 1/2.

Although defects in the 1973 OMF K1-model approach of Moynihan and associates [1973] have been pointed out for the last 10 years, papers continue to be published that use the OMF and ignore criticisms of it. It is therefore worthwhile to discuss it and its corrected version, the corrected modulus formalism (CMF), in order to make the issues involved clear to the reader, who can then make an informed choice between the two approaches. Although they both use the K1 response model, the OMF and CMF approaches are nevertheless crucially different.

Since the OMF response model was originally derived at the modulus level, let us begin by writing for the K0 model, $M_0(\omega) = i\omega\varepsilon_v\rho_0 I_0(\omega)$. In contrast, the OMF

analysis (Moynihan *et al.* [1973]) led to the following result for the $M_1(\omega)$ response of the K_1-model in terms of $I_0(\omega)$,

$$M_1(\omega) = i\omega\varepsilon_V\rho_0 I_1(\omega) = [1 - I_{01}(\omega)]/\varepsilon_Z \tag{1}$$

where ε_Z was defined as $\varepsilon_{D\infty}$, now written by supporters of the OMF as ε_∞. The subscript 01 is used here to indicate that $I_{01}(\omega)$ is just $I_0(\omega)$ in form but involves β_1 rather than β_0.

The OMF K1 model of Eq. (1), derived from a purely conductive-system correlation function, improperly mixes together conductive-system and dielectric-system responses through its identification of ε_Z as $\varepsilon_{D\infty}$. This identification leads to a world of problems (e.g. Macdonald [1996, 2002a, 2004]) vitiating this approach and implying that the OMF should be replaced by the CMF or by a superior model.

The CMF correction is simple: ε_Z in Eq. (1) is defined as the limiting dielectric constant $\varepsilon_{C1\infty} \equiv \varepsilon_{C1}(\infty)$, a purely conductive-system non-zero quantity associated only with charge-carrier motion and defined below. Except for the explicit introduction of ε_Z, the essence of the 1973 OMF derivation of Eq. (1) appeared in the earlier work of Macdonald and Barlow [1963]. Incidentally, for the K0 model, $\varepsilon_{C0\infty} \equiv \varepsilon_{C0}(\infty) = 0$. For both the K0 and CMF K1 models, one therefore needs to account for the endemic presence of $\varepsilon_{D\infty}$ by including a free dielectric-constant fitting parameter, ε_x, in the composite fitting model, now designated the CK0 model for K0 response and the CK1 for the CMF K1 situation. Then for the K0 model $\varepsilon_\infty = \varepsilon_x$, and for the CK1 $\varepsilon_\infty = \varepsilon_{C1\infty} + \varepsilon_{D\infty}$. The separate existence of $\varepsilon_{C1\infty}$ is not recognized by users of the OMF. Note that CK0 and CK1 fits of the same data lead to nearly the same estimates of ε_∞.

It has sometimes been found useful to replace the ideal capacitance represented by $\varepsilon_x = \varepsilon_{D\infty}$ by a parallel constant-phase element, the PCPE, $\varepsilon_{PC}(\omega) \equiv A_{PC}(i\omega)^{-\gamma_{PC}}$, with $0 \le \gamma_{PC} < 1$, reducing to a nearly ideal capacitance when $\gamma_{PC} << 1$ so that $A_{PC} \cong \varepsilon_{D\infty}$. The resulting composite model has been designated the PK1. A series CPE, the SCPE, $\sigma_{SC}(\omega) \equiv \varepsilon_V A_{SC}(i\omega)^{\gamma_{SC}}$ with $0 \le \gamma_{SC} \le 1$, has often been found satisfactory for modeling electrode effects, and it represents the effect at the complex resistivity level of a completely blocking series capacitance when $\gamma_{SC} = 1$. When SCPE response is combined with that of the CK1, the result is written as the CK1S model. For the data fitting described in the next section, it turns out that a more complicated model is needed to represent electrode effects more exactly.

The OMF K1 was derived by considering electric field decay at constant dielectric displacement and is thus a macroscopic response model. It has been shown, however, that the CMF K1, with $\varepsilon_Z = \varepsilon_{C1\infty}$, is completely isomorphic in form with the famous stochastic-transport microscopic analysis of Scher and Lax [1973a], a continuous-time, random-walk hopping model. The extended version of this model (Macdonald [2002d]) leads to response of exactly the form shown in Eq. (1), involving a quantity equivalent to $I_{01}(\omega)$ derived by Fourier transform from an initially unspecified correlation function associated with a waiting time distribution for hopping. It is the specific stretched-exponential choice for this function that leads to explicit K1 response. These considerations show that the K1 may be derived by considering either macroscopic or microscopic processes, and such generality possibly

accounts for the ability of the CK1 to fit a variety of conductive-system frequency-response data exceptionally well (e.g. Macdonald [2000b, 2002a, 2003a]).

The OMF expression for $\varepsilon_Z = \varepsilon_\infty$ may be written (Macdonald [1996, 2001c, 2002d])

$$\varepsilon_\infty = \sigma_0 \langle \tau \rangle_{01} / \varepsilon_V = \varepsilon_{Ma} \langle x \rangle_{01} = \varepsilon_{Ma} \beta_{1O}^{-1} \Gamma(\beta_{1O}^{-1}) \tag{2}$$

where the averages are over the resistivity DRT for the K1 model, and the OMF β_1 is designated as β_{1O} to distinguish it from that of the CMF, β_{1C}. Here the Maxwell quantity ε_{Ma} is

$$\varepsilon_{Ma} \equiv \sigma_0 \tau_o / \varepsilon_V \tag{3}$$

$x \equiv \tau/\tau_o$; and τ_o denotes the characteristic relaxation time of the K1 model, and it will be used for other models as well. The part of Eq. (2) involving the gamma function is only appropriate in the absence of cutoff of the K1 distribution of relaxation times (Macdonald [1996, 2001c]).

In contrast, for the CMF K1 dispersion model, $\varepsilon_Z = \varepsilon_{C1\infty}$, where

$$\begin{aligned} \varepsilon_{C1\infty} &= \varepsilon_{Ma} / \langle x^{-1} \rangle_1 = \varepsilon_{Ma} \langle x \rangle_{01} = \varepsilon_{Ma} \beta_{1C}^{-1} \Gamma(\beta_{1C}^{-1}) \\ &= \left[\gamma N (qd)^2 / (6 k_B \varepsilon_V) \right] / T = A/T \end{aligned} \tag{4}$$

and N is the maximum mobile charge number density; γ is the fraction of charge carriers of charge q that are mobile; and d is the rms single-hop distance for the hopping entity. The high-frequency-limiting effective dielectric constant, $\varepsilon_{C1\infty}$, associated entirely with mobile-charge effects, is likely to arise from the short-range vibrational and librational motion of caged ions.

Comparison of CMF equations with those of the Scher–Lax hopping model (Macdonald [2002d]) shows that the K1 mean relaxation time, $\langle \tau \rangle_{01} \equiv \tau_o \langle x \rangle_{01}$, is identical with the mean hopping time of the microscopic model, also defined as the mean waiting time for a hop. The term involving N in Eq. (4), not included in the OMF, is fully consistent with the Scher–Lax model predictions. In practice, fits of the same data with the OMF K1 and with the CK1 of the CMF approach lead to very different estimates of τ_o and of β_{1O} and β_{1C}.

We expect that the quantities in the square brackets of Eq. (4) are usually temperature independent, so the fitting parameter A is then itself independent of temperature. It follows that in the usual case where τ_o is thermally activated, $T\sigma_0$ is activated with the same activation energy (Macdonald [2002a]). The presence of the N term of Eq. (4) shows that as the ionic concentration approaches zero, $\varepsilon_{C1\infty} \to 0$ and so $\varepsilon_\infty \to \varepsilon_{D\infty}$, requiring that $\varepsilon_{Ma} \to 0$ as well, in accordance with CMF fit results. The situation is different for the OMF expression of Eq. (2), however. In this case, OMF fits show that both ε_∞ and ε_{Ma} approach the same constant value, that of $\varepsilon_{D\infty}$. There is then no dispersion, and the response reduces to that of single-time-constant Debye behavior.

Fits of frequency-response data for a variety of materials, temperatures, and concentrations lead to β_{1C} estimates all very close to 1/3. But OMF fits, particularly

of data in $M''(\omega)$ form, the usual OMF approach, invariably yield appreciably larger values of β_{1O}, ones that approach unity as the ionic concentration decreases or as the temperature increases. Such dependence led most users of the OMF to conclude that the correlation between charge carriers decreased as β_{1O} increased. But constancy of β_{1C} and the lack of Coulomb interactions in the well-fitting CMF microscopic model fail to support this supposition. For most data, it has been found that CK1 fits are superior to CK0 fits of the same data, but even in situations where these fits are comparable, CK1 ones are preferable to CK0 ones because $\beta_{1C} \cong 1/3$ estimates are virtually independent of temperature and ionic concentration, while CK0 β_0 estimates depend strongly on these variables (Macdonald [2002a, 2003a]).

Note that OMF data fitting with LEVM leads to estimates of the free parameters ρ_0, τ_o, and β_{1O}, and ε_∞ may then be calculated using Eq. (2). When β_{1C} is taken constant at the value of 1/3, CMF fits yield estimates of ρ_0, τ_o, and $\varepsilon_x \equiv \varepsilon_{D\infty}$, and $\varepsilon_{C1\infty}$ may then be calculated using Eq. (4), with $\varepsilon_{C1\infty} = 6\varepsilon_{Ma}$ for this value of β_{1C}. Although ρ_0 estimates are usually nearly the same for the two types of fits of the same data, as are also calculated values of ε_∞, β_{1O} is always appreciably larger than 1/3, and CMF τ_o estimates are generally at least an order of magnitude smaller than those from OMF fits.

When the OMF approach is used to fit experimental data, a fatal flaw appears, one that invalidates any conclusions based on such fitting results. For good data, all CMF fits yield closely the same estimates of τ_o and β_{1C}, independent of the immittance level for the data. This is not the case, however, for OMF fits. They lead to inconsistent results such that fits of the data in $M(\omega)$ or $M''(\omega)$ form yield characteristically large values of β_{1O}, usually falling in the range $0.45 \leq \beta_{1O} \leq 0.55$ for mid-range temperatures and concentrations, while fits of the same data in $\sigma'(\omega)$ form yield values close to 1/3. As mentioned earlier, since $\varepsilon_{D\infty}$ has no effect on $\sigma'(\omega)$ response, K1 and CK1 fits at this level must yield the same estimates, and OMF and CMF fits are then equivalent. A table of such comparisons and further discussion of OMF problems appear in Macdonald [2004] and make it evident that the OMF treatment of $\varepsilon_{D\infty}$ as an intrinsic part of the K1 dispersive conductive-system model is incorrect.

Coupling and Cutoff Models. The Ngai coupling model (Ngai [1979, 1998]), discussed in Macdonald [1998, 2005a], has been used in many conductive-system data analyses by Ngai and his associates. It assumes that for times longer than t_c (a temperature-insensitive cross-over time of the order of 1 ps) the temporal response of the system is of stretched-exponential character, and for shorter times it is of ordinary exponential character. In its applications to frequency response behavior, the coupling model has made use of OMF estimates of β_{1O}, although the frequency-response model directly corresponding to stretched-exponential behavior is the K0, not the K1, and generally $\beta_{1O} \neq \beta_0$.

A superior alternative, the cutoff model, avoids this inconsistency, makes no use of the OMF, and is based on a cutoff of the K1 distribution of relaxation times at $\tau = t_c$. It does not involve the OMF assumption that the correlation between charge carriers decreases as β_{1O} increases for response at frequencies below $\omega_c = 1/t_c$, and

it properly undergoes a transition to simple Debye response for frequencies greater than ω_c. Further, as shown in Macdonald [2005a], it leads not only to a smoother frequency-response transition around $\omega = \omega_c$ but also to satisfaction of the physical requirement that the K1 $\tau_o(T)$ never decreases below t_c as the measurement temperature becomes high. This requirement is not met by the $\tau_o(T)$ of the coupling model approach, suggesting that it should be superseded by the cutoff model. Both the coupling model and the cutoff one lead to non-Arrhenius behavior of $\sigma_0(T)$, with a transition from a low-temperature Arrhenius activation energy to a smaller apparent energy at high temperatures (Macdonald [1998, 2005a], León *et al.* [1998]).

Rationalization of the Barton, Nakajima, and Namikawa Relation. The Barton [1966], Nakajima [1972], and Namikawa [1975] empirical relation, usually designated by BNN, has played a useful role for some time in the analysis of dispersed frequency response data (e.g. Dyre [1988], Macdonald [1996], Dyre and Schrøder [2000], Porto *et al.* [2000]). It involves a loosely defined parameter, p, expected to be of order 1, and Nakajima and Namikawa believed that it arose from correlation between electrical conduction and dielectric polarization, apparently because it involved both measured dc conductivity and a dielectric strength quantity $\Delta\varepsilon$.

But as we have seen, for a conductive system both σ_0 and $\Delta\varepsilon = \varepsilon'(0) - \varepsilon'(\infty) = \varepsilon_0 - \varepsilon_\infty$ may arise entirely from mobile charge effects and not involve bulk dielectric effects at all. Then $\Delta\varepsilon = \Delta\varepsilon_{C1} \equiv \varepsilon_{C10} - \varepsilon_{C1\infty}$ for the CK1 model, and $\Delta\varepsilon = \Delta\varepsilon_{C0} \equiv \varepsilon_{C00}$ for the CK0 one. It was indeed pointed out by Macdonald [1996] that the K1 conducting-system model could lead to a quantitative value for p, one that depended on the value of β_{1C}.

Here it is shown that the BNN expression is most reasonably interpreted as arising entirely from charge motion, and if the K1 fit value of $\beta_{1C} = 1/3$ is a universal value, then the value of p is fully defined and the BNN equation is just a natural consequence of the apparent universal applicability or quasiuniversality of the conductive-system CK1 model with $\beta_{1C} = 1/3$. For ion-conducting homogeneous glasses and single crystals with charge motion allowed in all three dimensions it has been shown theoretically, in two independent ways that 1/3 is the only possible value of β_{1C} and that the resulting high-frequency-limiting-response power-law exponent is 2/3 (Macdonald [2005b], Macdonald and Phillips [2005]). Consistent with these results, it follows that CK0 model fits of such response lead to $\beta_0 = 2/3$ when the data extend to sufficiently high frequencies.

The BNN equation may be expressed as

$$\Delta\varepsilon = p^{-1}(\sigma_0/\varepsilon_V\omega_p) = p^{-1}(\tau_p/\tau_0)\varepsilon_{Ma} = p^{-1}(\nu_o/\nu_p)\varepsilon_{Ma} \tag{5}$$

Here as usual, τ_o is the characteristic response time of a fitting model such as the CK1. Further, $\omega_p \equiv 2\pi\nu_p = 1/\tau_p$, where ν_p is the frequency at the peak of the dielectric loss curve, $\varepsilon_s''(\nu)$, and $\nu_o \geq \nu_p$. For $\beta_{1C} = 1/3$, the K1 model leads to $\varepsilon_{C1\infty} = 6\varepsilon_{Ma}$ and to $\varepsilon_{C10} = 60\varepsilon_{Ma}$ (Macdonald [2001c, 2005b]). Therefore, $\Delta\varepsilon = 54\varepsilon_{Ma}$ and one may write for this situation $p = (\nu_o/\nu_p)/54$.

Sidebottom [1999] noted the similarity between the BNN equation and a scaling factor he proposed. This similarity arises because his result, appropriate for situa-

tions where the frequency response shape of the model is temperature independent, the situation for the K1 model with a constant $\beta_{1C} = 1/3$ value, is a simplification of scaling factors associated with K0 and K1 models with variable β_k, as discussed in Macdonald [2001c]. Of course with accurate CNLS fitting, scaling is unnecessary. The success of the Sidebottom scaling approach is further indirect evidence of the widespread applicability of the CMF CK1 model with fixed $\beta_{1C} = 1/3$.

From nearly exact calculations of K1 model $\varepsilon_s''(\omega)$ synthetic data derived from the parameter estimates of experimental data fits of the next section, with the electrode contributions present or removed, one finds that the ν_c/ν_p ratio is about 95 and 89, respectively, leading to p estimates of about 1.77 and 1.65. The 1.65 value is the appropriate one for K1-alone response and is universal to the degree that Eqs (1) and (4) are applicable and $\beta_{1C} = 1/3$. Although many data fits suggest that this value of β_{1C}, is a constant for CK1 fits, one would expect that as $\beta_{1C} \rightarrow 1$, p should also approach unity in the limit, and, for example, when $\beta_{1C} = 0.5$, one obtains $p \cong 1.27$.

Over the years since the introduction of the BNN equation, published p values have mostly fallen in the range of 0.5 to 10 but are often close to unity. Accurate estimation of p directly from experimental data is uncertain when electrode effects are significant and/or when the data range is too small to lead to good estimates of ε_0 and ε_∞. It is therefore appropriate to calculate p values from parameter values estimated from data fitting.

Although Hunt [1992] concluded that p cannot have a universal value, the present 1.65 value is consistent with most of the many BNN-related p estimates for experimental data presented by Dyre and Schrøder [2000] in their Figure 3, ones mostly slightly larger than unity. Such agreement is further evidence of the appropriateness of the CK1 model for many different materials. Earlier, Dyre [1988] quoted an estimate of p for a CTRW model different from the present Scher–Lax K1 one of only 0.42, while for their microscopic symmetric hopping model Dyre and Schrøder [2000] listed a value of 1.5 ± 0.4. The present results show that if CMF fitting is used, there is no need for the BNN since it is an automatic consequence of the applicability of such fitting. When CK1 CNLS fit parameters are available, however, the BNN equation with $p = 1.65$ may be used to obtain an accurate estimate of ν_p for the conducting-system part of the data alone.

Finally, Porto *et al.* [2000] have recently suggested that the BNN relation cannot apply for an appreciable range of concentrations because data fits show that $\Delta\varepsilon$ does not scale as N/T. But Eq. (4) shows that for the CMF K1 model $\varepsilon_{C1\infty}$ does indeed scale in this fashion and involves d^2 as well. Further, at constant β_{1C}, ε_{C10} and thus $\Delta\varepsilon$ also do so (Macdonald [2001c, 2002a]). Therefore, this criticism does not seem appropriate. To test the matter, estimates of p were calculated from CK1 CNLS fits of $x_c K_2O{\cdot}(1 - x_c)GeO_2$ germanate glasses with the relative ionic concentration, x_c, equal to 0.2 and 0.02, data kindly provided by Drs. Jain and Krishnaswami [1998]. The p estimates were 1.64 and 1.65, respectively, thus well verifying the appropriateness of the BNN equation over a considerable concentration variation.

Nearly Constant Loss Models. Nearly constant loss (NCL) is evidenced by a power-law dependence of $\sigma'(\omega)$ on frequency with an exponent very close to unity, leading to $\varepsilon_s''(\omega)$ loss response that varies only slightly over a substantial frequency

range. It may appear directly at low temperatures or may contribute significantly to $\sigma(\omega)$ response at the high end of the measured frequency range. In the first case, NCL is dominant and thermally activated hopping response is completely negligible (Macdonald [2001a, 2003b]. In the second case, hopping is dominant over most of the frequency range.

Excellent reviews and discussions of NCL behavior in ionically conducting glasses appear in Ngai [1999] and Roling *et al.* [2001]. Although most authors believe that NCL arises from the restricted motion of caged ions or groups of atomic species, very few quantitative NCL models have been proposed. An important early composite one may be written as $\sigma'(\omega) = \sigma_0[1 + (\omega\tau_o)^n] + A\omega^s$, with $0 < n \leq 1$ and $s \approx 1$ (Lee *et al.* [1991], Nowick *et al.* [1998]). The first term represents universal dynamic response, as discussed earlier, and constant loss occurs when $s = 1$, not a viable situation for a finite frequency range.

Although this composite model implies the additivity of hopping and NCL effects, the appropriateness of such additivity has been challenged by León *et al.* [2001] and Rivera *et al.* [2002]. They suggested an alternate serial (not series) picture in which NCL ceases to exist when hopping begins and ions begin to exit their cages. This is not a quantitative model, and their work dealt primarily with $\sigma'(\omega)$ response. Fitting of both synthetic and experimental complex data provides strong evidence, however, that additivity should not be rejected, and analysis using a quantitative complex model such as the PK1 suggests that hopping and NCL effects can exist simultaneously in a crossover region of finite length (Macdonald [2001a–c, 2002a]). Here, the parts of the model are in parallel electrically and additivity is ensured. The PCPE part of the expression models NCL behavior and can extend over an unrestricted frequency range.

Although a PCPE may be used to model NCL data with equal slopes for both $\sigma'(\omega)$ and $\varepsilon_s''(\omega)$ since they both involve the same $\gamma_{PC} << 1$ exponent, some data may be better represented by such power-law response for $\sigma'(\omega)$ but by a function that yields a very close approximation to constant loss for the $\varepsilon_s''(\omega)$ part of the response (Nowick *et al.* [1998]). In the absence of hopping, just the series combination of an ideal capacitor and a CPE can yield such behavior with very nearly constant loss over several decades of frequency (Macdonald [2001a]).

It was first shown in 2002 that the CPK1 composite model, where both C and a PCPE are in parallel with K1, could be used to represent frequency-independent undispersed $\varepsilon_{D\infty}$ behavior, hopping behavior, and NCL (Macdonald [2002a]). This work, in turn, suggested that the model could be made more physically plausible by an effective medium approach, one that might be able to represent both kinds of NCL behavior, as well as possibly non-negligible hopping effects. The resulting effective medium model, the EMK1, indeed met this objective well (Macdonald [2003b]). It is based on the assumption of a background involving a constant $\varepsilon_{D\infty}$ term and a volume fraction, η, of "inclusions" associated with ions vibrating over a limited region and represented by a PCPE. Thus, even in the absence of the K1 part, $\varepsilon_{EM}(\omega)$ is complex.

The EMK1 model, unlike the CPK1 one, leads to physically plausible low-frequency-limiting slopes for $\varepsilon(\omega)$ and other immittance functions, as well as equal

or superior fits to those of the CPK1. As a first approximation, η is set equal to the relative ionic concentration, x_c. Synthetic data for $\varepsilon''_{EM}(\omega)$ extending over many decades of frequency and for a wide range of η values showed that although there is no finite range of exact constant-loss behavior, such response is well approximated for η near 0.25. In addition, when the response is approximated by a power-law model, the resulting very small exponent may be either positive for $\eta << 1$ or negative for $\eta \geq 0.25$ over the higher-frequency region of the response.

There are two important questions arising from the present model discussions. First, a microscopic model needs to be developed that leads to $\beta_{1C} \cong 1/3$ and is less approximate than the Scher-Lax one and second, a microscopic model is also needed that yields response like the present effective medium model and takes explicit account of the detailed interactions, electromagnetic and otherwise, between vibrating ions and bulk dipoles.

4.2.3 Illustration of Typical Data Fitting Results for an Ionic Conductor

CNLS fitting has been little used by most workers who have analyzed frequency-response data for solid ionic conductors. The majority of published work deals primarily with either $\sigma'(\nu)$ or $M''(\nu)$ response, but not usually with both or with simultaneous fitting of real and imaginary parts of an immittance data set. An apparent advantage of the fitting and analysis of $\sigma'(\nu)$ data alone is that it and its direct transform, $\varepsilon''(\omega) \equiv \sigma'(\omega)/\omega\varepsilon_v$, are the only immittance-level parts that include no effects from $\varepsilon_{D\infty}$, as already mentioned in Section 4.2.2.1. But much more can generally be learned by considering full complex response at other immittance levels. Here we will only deal with data that do not extend to high enough frequencies or low enough temperatures to require a nearly constant loss contribution.

It is therefore worthwhile to illustrate, for a typical data set, the usefulness of CNLS fitting and of various plots of the results. For generality, the data set selected is one for which both bulk dispersion and electrode effects are non-negligible. It was kindly provided by Dr Carlos León and involves the fast ionic conductor $Li_{0.5}La_{0.5}TiO_3$, measured at T = 225 K (León *et al.* [1998]). This set is designated hereafter as LLTO.5. Fitting was carried out using the O circuit of the LEVM program. To allow independent work with this data set, its full LEVM input file, 225Z36EL, has been included in the LEVM FITTESTS folder of test files for the O circuit.

Figure 4.2.1 shows the full O circuit. For LEVM, only those circuit elements that are given non-zero values are used in fitting. Here "DE" designates a distributed circuit element, one that can be selected from a large number of different elements available in LEVM. DED involves a dielectric distributed element, such as the DSD, a dielectric-system dispersive element. Similarly, DEC designates a conductive distributed element, such as the CSD. In LEVM, the series inductance shown in the figure may be replaced by a short circuit, a resistor, or a capacitance, C_S.

Since it was initially established that the LLTO.5 data sets for different temperatures involved thermally activated response and were therefore of CSD charac-

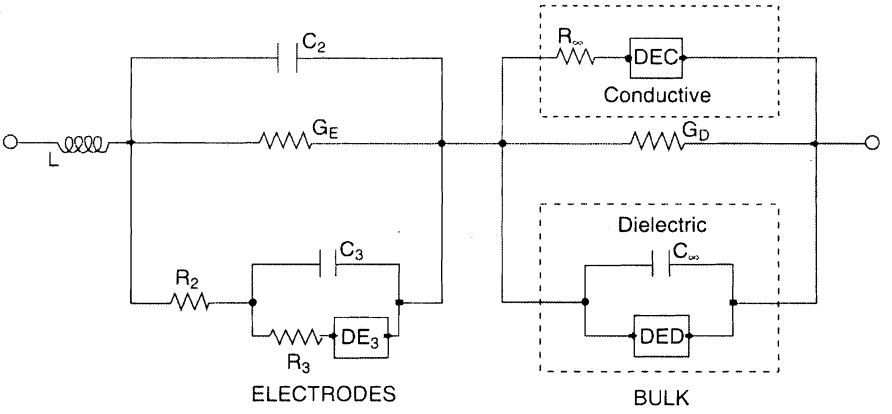

Figure 4.2.1. The LEVM fitting circuit O. It may be used as shown for fitting immittance data in raw or specific form. The DE blocks may each be selected as any one of the many available distributed-circuit-element response models.

ter, we begin by carrying out CMF fits of the T = 225 K data. The bulk response was thus represented by the K1 model in the DEC part of the circuit. It involves the parameters ρ_0, τ_o, and β_{1C}, but, as usual, a β_{1C} value of 1/3 yielded best results. Therefore, this value was taken as fixed for all the present fits. When the CMF CK1 model was employed, $\varepsilon_{D\infty}$ was represented by the C_∞ element of the circuit. As usual, R_∞ was found to contribute nothing to the fits and was thus not used thereafter.

For blocking electrodes the simplest element to represent their effect is a series capacitance, C_S, but electrode processes are generally too complicated for adequate representation by a single capacitance. The next level of complexity, often found adequate, is to use a series constant-phase element, the SCPE, in the DE_3 position of the circuit. A recent analysis of the use of a CPE for modeling electrode behavior appears in Bisquert *et al.* [1998]. For the present data, for which electrode effects are far from negligible, it was found that they were best represented by a SCPE in parallel with the C_3 capacitance of the circuit, all in series with C_S, involving a total of four free fitting parameters. The full CK1 model including these free electrode-related parameters is termed the CK1EL and involves a total of seven free parameters.

The CK1EL CNLS fit of the data at the complex resistivity level using LEVM with proportional weighting led to the estimates $\varepsilon_{D\infty} \cong 83.08$, $\rho_0 \cong 1.784 \times 10^5$ ohm-cm, and $\tau_o \cong 4.488 \times 10^{-8}$ s. In addition, the estimate for the γ_{SC} parameter of the SCPE was about 0.641. The fit also led to the estimates $\varepsilon_0 \cong 254$, $\varepsilon_{C10} \cong 171$, $\varepsilon_{C1\infty} \cong 17.1$, $\varepsilon_\infty \cong 100$, and $\Delta\varepsilon = \Delta\varepsilon_{C1} \cong 154$. Exactly the same parameter values were obtained for proportional-weighting fitting at the complex modulus level. The relative standard deviation of the overall fit, S_F, was 0.0072, indicating an excellent result.

When electrode effects were represented only by a SCPE, the CK1S model, S_F increased appreciably to 0.015. This fit led to a larger γ_{SC} estimate of about 0.897 and to the slightly different estimates for $\varepsilon_{D\infty}$, ε_0, ε_{C10}, $\varepsilon_{C1\infty}$, ε_∞, and $\Delta\varepsilon$ of about 79,

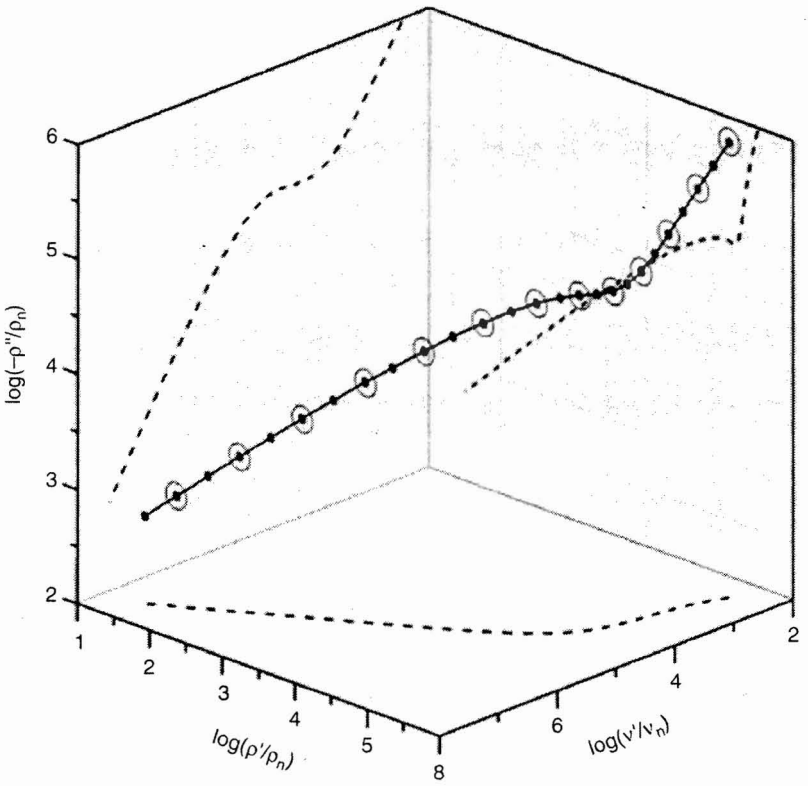

Figure 4.2.2. Three-dimensional log–log–log plot, with planar projections. The solid lines and solid circles show the data, and open circles identify points from CK1EL-model CNLS fitting of the $Li_{0.5}La_{0.5}TiO_3$ data (denoted LLTO.5 hereafter) at the complex resistivity level. The quantities with a subscript "n" in the axes names of this and subsequent figures are of unity magnitude and are included to make the arguments of the logarithms dimensionless as they should be.

254, 175, 17.5, 97, and .157, respectively. In the limit of low frequencies, the four-parameter model for electrode behavior is dominated by the blocking capacitor, C_S. Its value, expressed in dielectric-constant form was more than 30 times larger than the CK1EL estimate of ε_0.

Figure 4.2.2 presents a 3-D log–log–log plot of complex-resistivity data as well as fit points for the CK1EL model fit. The projections in the three planes involve only the data. The 3-D line shows every other one of the data points and every fourth fit point. Since the open-circle fit points enclose their corresponding data points symmetrically, no deviations are evident. The projection lines at the two back planes clearly show the transition to electrode-related power-law behavior toward the low end of the frequency scale. Space restrictions preclude presentation here of the three other 3-D immittance plots.

Figure 4.2.3 shows the behavior of the real and imaginary parts of the complex modulus. In addition to the CK1EL-fit lines, those for the CK1 and K1 parts of the

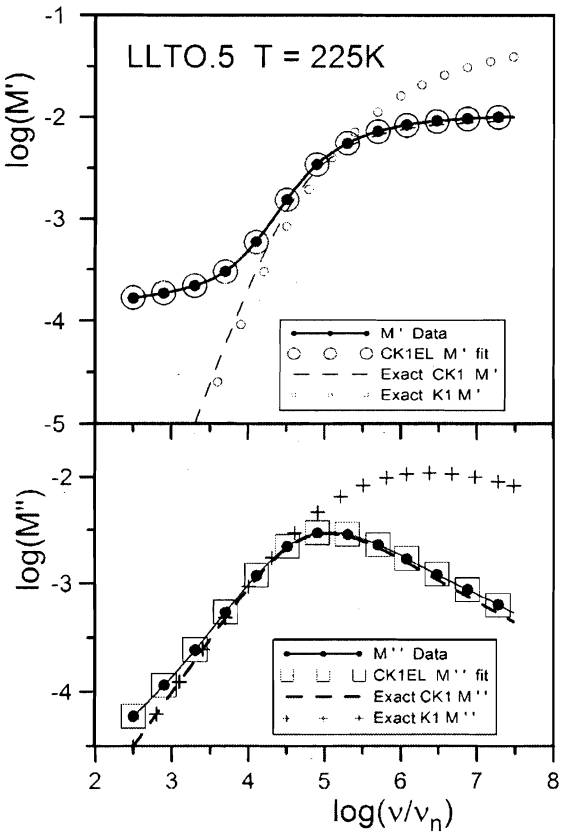

Figure 4.2.3. Log–log complex modulus data and fit results for $M'(\omega)$ and $M''(\omega)$ obtained from fitting the $M(\omega)$ complex data with the CK1EL model. In addition, predictions for the CK1 and K1 parts of the full model are shown.

model are also shown. They were calculated using, in LEVM, the appropriate parameter values found from the full CK1EL fit, and thus they are virtually exact representations of the model behavior for these values. The present M' results show that electrode effects are dominant at low frequencies and have only a minor effect at the high-frequency end of the data range. As one would expect, the difference between the CK1 and K1 results, associated entirely with $\varepsilon_{D\infty}$, becomes great at the high-frequency end.

It is often been stated that a virtue of plotting and analyzing data in M'' form is the resulting suppression of electrode effects. The present results demonstrate such suppression near the M'' peak, but it clearly diminishes as the frequency departs from the peak value. Further, since the same parameter estimates are obtained for both $\rho(\omega)$ and $M(\omega)$ fits when proportional weighting is employed, the suppression is graphical but not significant for least-squares fitting. Finally, it is evident that the peak of the K1 M'' curve appears at much higher frequencies than that of the data

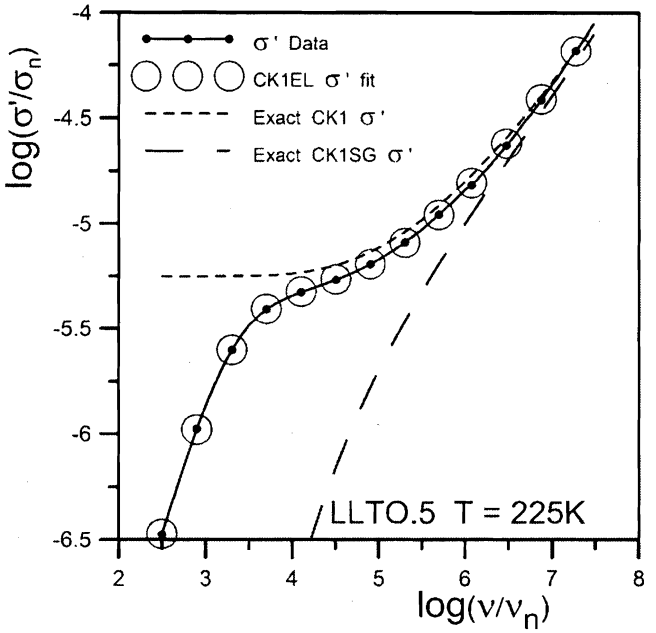

Figure 4.2.4. Log–log $\sigma'(\omega)$ data and fit results from CNLS fitting as in Figure 4.2.3. The CK1SG results eliminate both electrode effects and those of σ_0.

and the CMF CK1 one and the breadth of the K1 curve at half height is also much larger. This difference is associated with the CK1 value of β_1 of 1/3 and a value greater than 0.5 found for OMF fitting of the $M(\omega)$ data, as expected from the discussion in Section 4.2.2.

Figure 4.2.4 compares $\sigma'(\omega)$ data and CK1EL fit values, as well as individual contributions to the full model. For this immittance level, there is no effect from $\varepsilon_{D\infty}$, so here CK1EL and K1EL fit results are equivalent. The CK1SG results were obtained by first setting the G_D parameter of the Figure 4.2.1 circuit to $-\sigma_0$. This, together with the K1 parameter estimates obtained from the CK1EL fit, were then used in LEVM to calculate the resulting exact response of the combination and thus to eliminate the effect of σ_0. It is evident that, as expected, at the high frequency end of the range the $\sigma'(\omega)$ response is nearly entirely associated with the ac part of the K1 model, with only a small contribution from electrode effects apparent. Further, the data curve shows that no accurate value of σ_0 could be directly estimated from it, making it essential that all fits should account for electrode effects.

Rather than present $\sigma''(\omega)$ fitting results, it is appropriate to show those for the corresponding $\varepsilon'(\omega)$, related to $\sigma''(\omega)$ by a factor of $1/\varepsilon_V\omega$. Such results are presented in the top part of Figure 4.2.5. It is clear that the $\varepsilon'(\omega)$ data curve alone does not allow one to obtain a reasonable estimate of ε_0 from it. Removal of the electrode effects obtained from the full CK1EL fit leads to the low- and high-frequency plateau values ε_0 and ε_∞, respectively, while subsequent removal of $\varepsilon_{D\infty}$ leads to the limiting conductive-system K1-model quantities ε_{C10} and $\varepsilon_{C1\infty}$. It is again evident that elec-

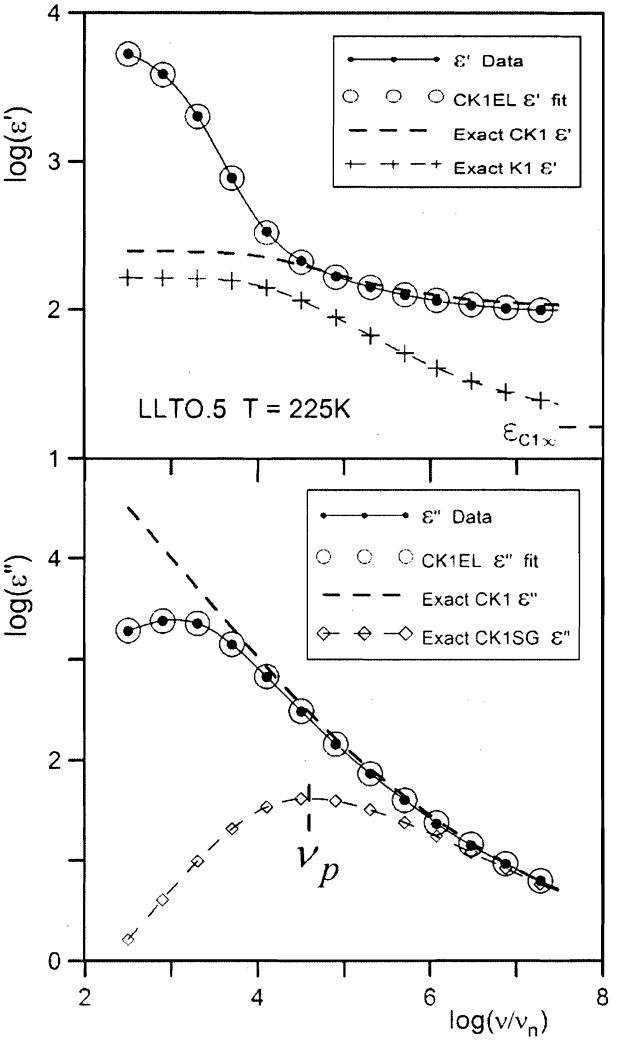

Figure 4.2.5. Log–log $\varepsilon(\omega)$ data and fit results from CNLS fitting as in Figure 4.2.3. The exact CK1 response is that without electrode effects, and the K1 response eliminates the effect of $\varepsilon_{D\infty}$ as well and shows the approach of the data toward the limiting $\varepsilon_{C1\infty}$ value. The peak of the CK1SG $\varepsilon_s''(\omega)$ curve is denoted by ν_p.

trode effects play a minor but not completely negligible role at high frequencies. The bottom part of the present figure shows $\varepsilon''(\omega)$ results, where again $\varepsilon_{D\infty}$ plays no role. The frequency at the peak of the CK1SG curve, that for $\varepsilon_S''(\omega)$, is shown by ν_p and is needed for the calculation of the BNN quantity p.

Finally, Figure 4.2.6 is a linear-scale complex-resistivity-plane plot. Here, to allow greater resolution, lower-frequency points than those shown have been

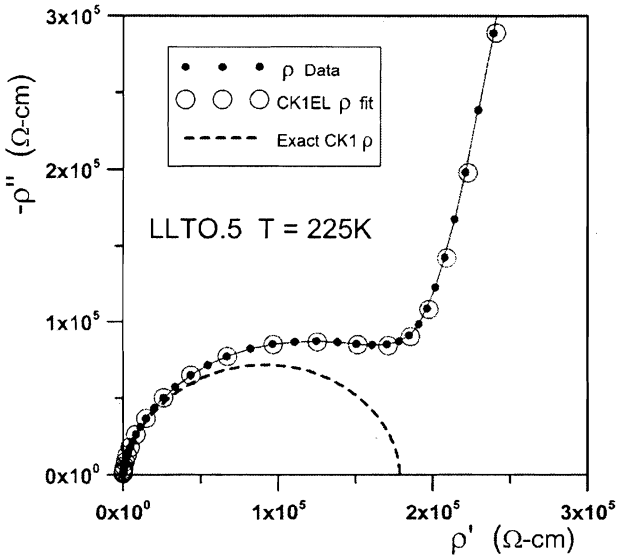

Figure 4.2.6. $\rho(\omega)$ data and fit results from CNLS fitting as in Figure 4.2.2. These complex-plane results demonstrate clearly the dominance of electrode effects up to quite high frequencies.

omitted. The results indicate that electrode effects remain important over much of the frequency range, even toward the higher frequencies. Comparison of corresponding data and fit points shows some very minor discrepancies for the spur part of the response, ones that are too small to be evident in log–log plots. The low-frequency end of the CK1-only part of the response approaches the axis at 90° as it should and defines the value of ρ_0. It is important to note that extrapolation of the electrode spur line down to the ρ' axis leads directly to an excellent estimate of ρ_0. This can be useful when the temperature is so high that little or none of the bulk arc is included in the measurement range and CNLS fitting may not have been carried out. However, such extrapolation fails for mixed ionic and electronic conduction situations.

In a full data analysis, one would first determine the most appropriate model and then use it to carry out fits for each different temperature available. Here, only partial results for fits of the present T = 225 K data with a few other models will be discussed. First, S_F values for CNLS proportional weighting fits with the CK0EL, OMF K1EL, and "DSD" EDAEEL models were all close to 0.007; excellent fits. Here, the EDAE model involves an exponential distribution of activation energies fitted at the complex dielectric level and assuming dielectric-system dispersion. Since the fits were all comparable, selection of a best model must depend on other criteria.

The CK0EL model led to CNLS estimates of ε_0, $\varepsilon_{C10} = \Delta\varepsilon$, and ε_∞ of about 255, 145, and 97, respectively. Since this model always involves $\varepsilon_{C0\infty} = 0$, it does not

yield a separate estimate of $\varepsilon_{D\infty}$, but its β_0 and γ_{SC} estimates were about 0.487 and 0.635, respectively. Note that with $\beta_{1C} = 1/3$, $\beta_0 + \beta_{1C} \neq 1$ here. Even when the CK1EL and CK0EL models yield comparable fits and nearly the same estimates for some common parameters, the former, with fixed $\beta_1 = 1/3$, should be preferred because it yields not only a comparable fit with fewer free parameters but because it also leads to separate estimates of both $\varepsilon_{C1\infty}$ and $\varepsilon_{D\infty}$.

For the OMF K1EL model, $\varepsilon_0 = \varepsilon_{C10}$, $\Delta\varepsilon$, and $\varepsilon_\infty = \varepsilon_{C1\infty}$ values were all calculated from the CNLS fit parameters, leading to estimates of about 233, 118, and 115, respectively. They thus agree less well with the CK1EL and CK0EL fit results. The above $M(\omega)$ fit results used proportional weighting, but $M''(\omega)$ NLS fits with either proportional or unity weighting led to closely similar estimates. The β_{1O} and γ_{SC} values estimated for these fits were about 0.604 and 0.607, respectively. Finally, an OMF K1EL fit of the $\sigma'(\omega)$ part of the data, with electrode parameters fixed at their K1EL $M(\omega)$-fit values, led to ε_0, $\Delta\varepsilon$, and ε_∞ estimates of about 175, 156, and 18.5, respectively. The last value is clearly an estimate of the CK1 $\varepsilon_{C1\infty}$ quantity here. Further, the β_{1O} estimate was 0.338, very close to the fixed value of 1/3 for the CK1EL fitting. The stark inconsistency between the OMF $M(\omega)$ and $\sigma'(\omega)$ β_{1O} estimates, also observed in all other such published comparisons, is a clear indication of the failure of the OMF to take proper account of $\varepsilon_{D\infty}$. Therefore, it is a particularly inappropriate fitting model and should not be used.

Although the present data involve CSD rather than DSD behavior, it is of interest to fit at the dielectric level with a DSD model, one that involves a ρ_0 parameter separate from the dispersion model. The asymmetric EDAE model, available in LEVM, is appropriate for this situation and involves the bulk parameters $\Delta\varepsilon$, ε_∞, τ_0, and γ_E, where γ_E falls in the range $0 < \gamma_E \leq 1$. CNLS fitting using the EDAEEL model with proportional weighting led to estimates of the above quantities of 131, 109, 9.11×10^{-6} s, and 0.473, respectively. The prediction for ε_0 is therefore 240 and the estimate for ρ_0 was 1.73×10^5 ohm-cm.

The standard deviations of parameters common to both the CK1EL and EDAEEL fits were appreciably larger for the latter than for the former even though their overall S_F values were nearly the same. Not only does the EDAEEL model involve two more free parameters than does the CK1EL one, but its separate treatment of ρ_0 is inappropriate for a CSD situation. The present results clearly indicate that for the LLT0.5 CSD data, and probably for most such data, the CK1 model with $\beta_1 = 1/3$ is the most appropriate bulk fitting and analysis model. Its BNN p value was found to be 1.65, as was that for the EDAE fit, and that for the K0 was about 1.33.

4.3 SOLID STATE DEVICES

William B. Johnson
Wayne L. Worrell

In this section examples of several different applications of impedance spectroscopy (IS) will be presented. Four different devices have been chosen: solid electrolyte